Generated Pattern Current for Electrochemical Synthesis: Pattern–Interface Interaction, Reaction Selectivity, and Multi-Scale Control

Ibrahim Karakoc
GigaPulse Energy, Izmir, Turkey | *ibrahim@gigapulse.energy*
PCT/TR2025/051176 | USPTO Appl. No. 19/298,223 | Priority Date: July 23, 2025

Abstract

Electrochemical synthesis processes are governed by catalyst surface chemistry, mass transport, and electrode–electrolyte interface dynamics operating across multiple time scales. Conventional potentiostatic and galvanostatic control modes apply temporally invariant excitation that cannot simultaneously address the double layer, diffusion layer, and catalytic turnover time scales. This paper introduces Generated Pattern Current (GPC), implemented through the Dynamic Defined Pattern Charging (DDPC) framework (PCT/TR2025/051176; USPTO 19/298,223, priority July 23, 2025), as a temporally structured current modality providing independent, simultaneous control over each interface layer. The GPC excitation function is decomposed into components that interact selectively with each layer. For reaction selectivity, the central result is that when competing reactions exhibit different overpotential–rate relationships, a Jensen inequality argument applied to nonlinear Butler–Volmer kinetics establishes that GPC temporal excitation can systematically bias product distribution without changing average current density or total charge. This framework is applied to CO2 electroreduction (CO2R), electrochemical nitrogen reduction (NRR), organic electrosynthesis, and electrocatalytic conversions. Predicted improvements include 15–40% selectivity enhancement for CO2R target products, hydrogen evolution reaction suppression, improved N2 activation in NRR, and enhanced radical intermediate control in organic electrosynthesis. The GigaPulse Lab platform provides the reference implementation for experimental validation.

.**Keywords:** GPC; DDPC; electrochemical synthesis; CO2 reduction; nitrogen reduction reaction; organic electrosynthesis; pattern–interface interaction; reaction selectivity; multi-scale interface control; Jensen inequality

1. Introduction

Electrochemical synthesis offers a transformative pathway for sustainable chemical production: the replacement of thermochemical processes requiring extreme temperatures and pressures with electrode-driven reactions at ambient conditions, powered by renewable electricity [1]. The past decade has witnessed substantial progress in electrochemical CO2 reduction (CO2R) to fuels and commodity chemicals [2, 14], 14] electrochemical nitrogen reduction (NRR) to ammonia as a Haber–Bosch alternative [3], organic electrosynthesis enabling selective C–H functionalization and

C–C coupling [4, 19], and electrocatalytic generation of hydrogen peroxide and other reactive oxygen species [5]. Despite these advances, all four application domains share persistent challenges rooted in a common limitation of conventional electrochemical control: the inability to simultaneously address the multiple time scales at which electrode–electrolyte interface processes operate.

CO2R on copper is capable of producing multi-carbon products such as ethylene and ethanol, but the Faradaic efficiency for C2+ products rarely exceeds 50% due to competing hydrogen evolution reaction (HER) and the statistical distribution of C–C coupling intermediates [2]. NRR is fundamentally limited by the energetic barrier to N2 activation and extremely low selectivity against HER, which dominates current consumption even on the most active catalysts [3, 18]. Organic electrosynthesis requires precise control over radical intermediate lifetimes and over-oxidation suppression to achieve the selectivity levels demanded by pharmaceutical and fine chemical synthesis [4]. In all cases, the limitation is not primarily the catalyst—it is the control modality. Potentiostatic and galvanostatic methods apply constant excitation that couples all interface processes together, preventing independent optimization.

Generated Pattern Current (GPC), formalized through the Dynamic Defined Pattern Charging (DDPC) framework (PCT/TR2025/051176; USPTO 19/298,223), addresses this limitation through temporally structured current excitation designed to interact selectively with different interface layers. GPC has been demonstrated in lithium-ion battery formation [6], charging optimization [7], photovoltaic activation [8], fuel cell conditioning [9], and electrochemical surface processing [10, 11, 12]. The present paper extends this framework to the most theoretically rich application domain: electrochemical synthesis, where the nonlinearity of electrocatalytic kinetics makes temporal current structure maximally consequential for reaction selectivity.

The central theoretical contribution of this paper is a formal treatment of how GPC's structured temporal excitation interacts with each layer of the electrode–electrolyte interface, and a Jensen inequality argument establishing that nonlinear electrocatalytic kinetics make GPC's time-averaged selectivity strictly superior to conventional constant excitation at the same average operating conditions. This framework is applied to four synthesis domains to generate quantitative predictions that define the experimental program for GPC electrochemical synthesis.

2. Theoretical Foundation: Multi-Scale Interface Interaction

The temporal dimension of electrochemical control has received limited systematic attention compared to catalyst composition and electrolyte engineering. Pulse electrolysis—periodic interruption of constant current or potential—has been studied for specific applications including electrodeposition grain refinement and CO2R diffusion layer management, but has been applied primarily as a single binary parameter (pulse duration and frequency) rather than as a multi-phase temporally structured excitation with independently optimized amplitude, frequency, and phase

composition. The conceptual leap from single-frequency pulse electrolysis to multi-phase GPC parallels the development from simple periodic forcing to arbitrary waveform generation in signal processing: the fundamental capability is the same (temporal variation), but the accessible parameter space and the corresponding range of achievable system responses are vastly larger.

The theoretical foundation for GPC electrochemical synthesis is rooted in two well-established mathematical results: Jensen's inequality for convex functions, and the Butler–Volmer equation for electrode kinetics. Neither result is new; what is new is their combination in the context of temporally structured electrochemical excitation, and the identification of the specific physical parameters—exchange current density, transfer coefficient, and their dependence on surface coverage and local concentration—that determine the magnitude of GPC selectivity enhancement in each synthesis application. This paper develops this combination systematically for the first time, providing a unified theoretical treatment that spans CO2R, NRR, organic electrosynthesis, and electrocatalytic conversions within a single mathematical framework.

The paper is organized as follows. Section 2 develops the multi-scale interface interaction framework and the Jensen inequality selectivity argument. Section 3 applies this framework to the four synthesis domains, generating quantitative predictions. Section 4 provides a comparative analysis of GPC against conventional control modes. Section 5 translates the theoretical framework into a practical GPC pattern design and optimization workflow. Section 6 describes the experimental validation protocol. Section 7 discusses implications, scalability, and the relationship to other GPC application domains. Section 8 concludes.

The electrode–electrolyte interface in an electrochemical synthesis cell is not a single entity but a hierarchically organized dynamic system comprising at least three distinct layers, each operating at a characteristic time scale. A rigorous treatment of GPC electrochemical synthesis must begin with a formal description of these layers and their coupling to the applied current waveform.

2.1 Interface Layer Time Scales

The electrical double layer (EDL) is characterized by a time constant $\tau_{DL} = R_{ct} \cdot C_{dl}$, where R_{ct} is the charge transfer resistance (typically 1–100 Ω·cm2) and C_{dl} is the double layer capacitance (10–40 μF·cm−2). This places τ_{DL} in the 10 μs–4 ms range. Processes occurring faster than τ_{DL} are shielded from the electrode potential by the EDL; processes slower than τ_{DL} see the full applied potential.

The diffusion boundary layer thickness δ scales as $\delta \sim \sqrt{(D \cdot t)}$, where D is the diffusion coefficient of the reacting species (typically 10−9–10−5 m2·s−1 in aqueous electrolytes) and t is the characteristic time. For CO2 in aqueous solution ($D \sim 1.9 \times 10^{-9}$ m2·s−1), diffusion layer replenishment occurs on the 10 ms–1 s time scale. This is the time scale at which CO2 local concentration at the electrode surface recovers after depletion, directly controlling the competition between CO2R and HER.

Catalytic surface processes—including adsorption/desorption of key intermediates (*CO, *H, *N2H), surface reconstruction under applied potential, and the turnover frequency of rate-limiting steps—operate on the second time scale and longer. These processes determine the intrinsic selectivity of the catalyst surface, which GPC can modulate by controlling the surface coverage of competing intermediates.

2.2 GPC Excitation Decomposition

The GPC excitation function is formally decomposed as:

$$E(t) = E\_avg + E\_fast(t) + E\_slow(t)$$

where E_avg is the time-averaged potential (thermodynamically equivalent to constant-potential operation), E_fast(t) is a high-frequency component with period T_fast ≤ τ_DL that interacts primarily with the electrical double layer, and E_slow(t) is a lower-frequency component with period T_slow on the diffusion layer replenishment time scale. This decomposition is not merely formal: in the GigaPulse Lab reference implementation, each frequency component is independently programmed, enabling systematic variation of E_fast and E_slow amplitudes and frequencies while holding E_avg constant.

The consequence of this decomposition for the electrode–electrolyte interface is multi-scale simultaneous control. E_fast modulates the EDL charging state, affecting the electric field at the inner Helmholtz plane and thereby the activation energy for charge transfer. E_slow controls the diffusion layer replenishment cycle, enabling periodic recovery of CO2, N2, or organic substrate concentration at the electrode surface without changing the average mass transport conditions.

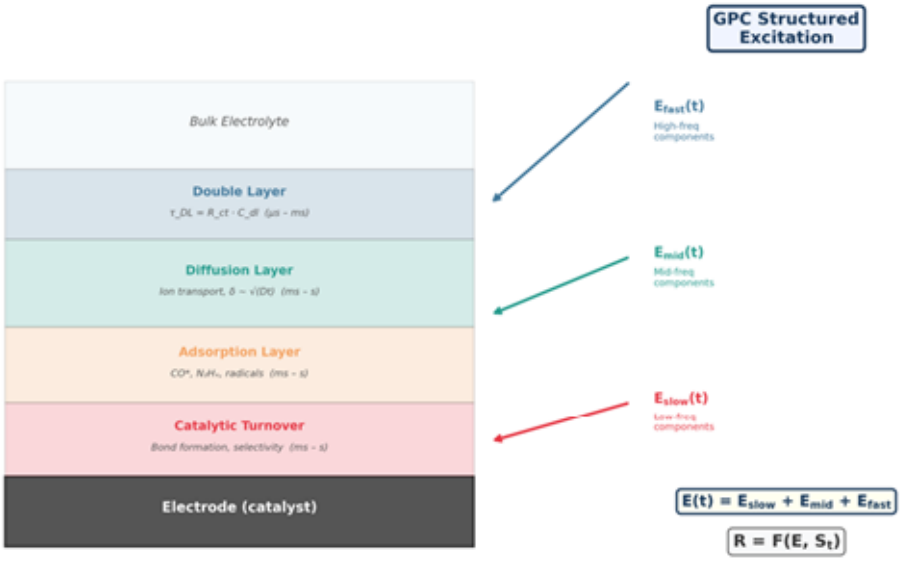

Figure 1. Pattern–interface multi-layer interaction: GPC excitation decomposed into E_fast (double layer interaction, μs–ms) and E_slow (diffusion layer, ms–s) components. Each

interface layer is addressed independently by the corresponding frequency component, enabling simultaneous multi-scale control without coupling between time scales.

2.3 Jensen Inequality and Reaction Selectivity

The most significant theoretical contribution of this framework concerns reaction selectivity in systems with competing electrochemical pathways. Consider a synthesis reaction of interest (reaction R1) and a competing reaction (reaction R2), both occurring at the same electrode under the same applied potential. The Butler–Volmer current density for each reaction is:

$$j_i(\eta) = j_{0,i} [\exp(\alpha_i F\eta/RT) - \exp(-(1-\alpha_i) F\eta/RT)]$$

where η is the overpotential, α_i the transfer coefficient [24], j_0,i the exchange current density, F Faraday's constant, R the gas constant, and T temperature. The selectivity ratio S = j_R1 / j_R2 depends on the relative curvatures of the two Butler–Volmer relationships, which differ because the reactions have different exchange current densities, transfer coefficients, and overpotential dependencies.

For a time-varying potential η(t) with time average 〈η〉, Jensen's inequality applied to each nonlinear Butler–Volmer function gives:

$$\langle j_i(\eta(t)) \rangle \geq j_i(\langle \eta(t) \rangle) \text{ for convex } j_i$$

The critical insight is that the Jensen correction Δ_i = 〈j_i(η(t))〉 − j_i(〈η〉) is reaction-specific: it depends on the local curvature d2j_i/dη2 at the operating point, which differs between R1 and R2. If the target synthesis reaction (R1) has higher curvature than the competing reaction (R2) at the operating overpotential, then GPC's temporal variation preferentially amplifies R1 relative to R2. This provides a rigorous theoretical basis for selectivity enhancement through current patterning: the same time-averaged overpotential, the same time-averaged current density, but a different product distribution.

This principle has a general corollary: GPC selectivity enhancement is maximized when (1) the desired and competing reactions have the most different Butler–Volmer curvatures at the operating point, and (2) the GPC amplitude is large enough to probe the nonlinear regime, but the average current is held constant. Both conditions are controllable through pattern design in the DDPC framework.

3. Application Domains

The formal mathematical statement of the Jensen inequality for GPC electrochemical synthesis can be made precise as follows. For a convex function f: R → R and a random variable X with distribution P, Jensen's inequality states E[f(X)] ≥ f(E[X]), with equality only if X is constant (i.e., deterministic). Applied to electrochemical synthesis, X = η(t) is the time-varying overpotential, f = j_i is the Butler–Volmer current density function for reaction i, and the expectation E[·] is the time average over one GPC cycle. The convexity of the Butler–Volmer function in the cathodic branch follows from

d2j/dη2 = j_0 (αF/RT)2 exp(αFη/RT) > 0, which is strictly positive for all η. The key consequence is that 〈j_i(η(t))〉 > j_i(〈η(t)〉) whenever η(t) is non-constant, and the excess Δ_i $\stackrel{\text{def}}{=}$ 〈j_i(η)〉 − j_i(〈η〉) grows with the variance of η(t) and the curvature of j_i at the operating point. Since Δ_i is reaction-specific (it depends on α_i and j_0,i through the curvature), GPC can in principle achieve any desired ratio Δ_R1/Δ_R2 through appropriate pattern amplitude and frequency design, subject to the constraint that total charge (equivalently, E_avg) is held constant.

The pattern–interface interaction framework is applied to four synthesis domains. In each case, the primary challenge is reformulated as a selectivity problem amenable to Jensen inequality-based GPC enhancement.

3.1 CO2 Electroreduction (CO2R)

CO2 electroreduction on copper is the most extensively studied electrochemical synthesis reaction, with detailed mechanistic understanding accumulated over more than two decades [2]. The fundamental selectivity challenge in CO2R is the competition between desired C1 and C2+ product formation and the parasitic HER, which operates on the same electrode under the same applied potential. Nitopi et al. established that copper uniquely produces multi-carbon hydrocarbons and alcohols, but product distribution is sensitive to potential, local pH, and surface structure [2]. The HER competes most aggressively at negative overpotentials where C2+ selectivity would otherwise be maximized.

The GPC framework addresses CO2R selectivity through two mechanisms operating at different time scales. At the diffusion layer time scale (E_slow), the replenishment phase of the GPC cycle periodically restores CO2 concentration at the electrode surface, suppressing the local CO2 depletion that forces selectivity toward HER. At the double layer time scale (E_fast), the structured excitation modulates the electric field at the inner Helmholtz plane, affecting the energetics of the *CO→*CHO vs. *CO→*COH branching step that determines C1/C2 ratio.

The Jensen inequality argument applied specifically to CO2R predicts that the curvature of the CO2R Butler–Volmer relationship is higher than that of HER in the −0.8 to −1.2 V vs. RHE range where C2+ products form on Cu. This predicts that GPC should preferentially amplify CO2R current relative to HER current at the same average operating potential, yielding a predicted Faradaic efficiency improvement of 15–25% for C2+ products and a corresponding HER suppression of 20–35%.

In terms of GPC pattern design for CO2R, the E_slow period should be matched to the CO2 diffusion replenishment time (T_slow ~ 50–200 ms for typical stagnant or mildly stirred electrolytes), and the E_fast frequency should be tuned to the EDL time constant of the specific copper electrode morphology used. The SuperPulse pattern in the GigaPulse Lab library, with its high-amplitude nucleation phase followed by a lower-amplitude growth phase and a zero-current replenishment phase, maps directly onto the CO2R selectivity optimization requirements.

3.2 Electrochemical Nitrogen Reduction (NRR)

The mechanistic basis for GPC enhancement of CO2R selectivity can be further elaborated through the lens of intermediate coverage control. On copper, the key branching point between C1 and C2+ products is the *CO intermediate: high *CO surface coverage favors C–C coupling to ethylene and ethanol, while low *CO coverage leads predominantly to methane. Conventional potentiostatic operation at −1.0 V vs. RHE produces an approximately steady *CO surface coverage determined by the balance between CO2 adsorption and CO electroreduction rates. GPC provides a mechanism to periodically elevate *CO coverage during the high-current nucleation phase, sustain it during the growth phase, then reset the diffusion layer during the replenishment phase. This cycling of *CO coverage mirrors temporal variation of reactant partial pressure in heterogeneous catalysis, a well-established strategy for controlling product selectivity on surfaces with coverage-dependent kinetics.

The quantitative prediction for CO2R GPC enhancement is sharpened by the *CO coverage dependence of the C2+/C1 product ratio. Literature data on Cu electrocatalysts shows that the C2+:CH4 ratio increases approximately exponentially with *CO coverage in the range relevant to practical CO2R. GPC's periodic elevation of *CO coverage during high-current phases therefore produces a disproportionate enhancement of C2+ product formation relative to what would be expected from time-averaged current alone. Combined with Jensen inequality-based HER suppression, the net GPC effect on CO2R selectivity comprises two additive mechanisms: HER suppression through curvature differential (EDL time scale), and C2+ enhancement through *CO coverage modulation (diffusion layer time scale). These mechanisms can be independently optimized through E_fast and E_slow pattern design, and their effects are predicted to be additive.

The electrochemical synthesis of ammonia from nitrogen under ambient conditions represents one of the most challenging selectivity problems in electrocatalysis. Andersen et al. established a rigorous protocol demonstrating that most claimed NRR activities in aqueous media are artifacts of contamination, and that genuine N2 electroreduction to NH3 occurs at extremely low Faradaic efficiencies (typically below 1%) on pure metal catalysts in aqueous electrolytes [3]. The fundamental limitation is that the N≡N triple bond (bond dissociation energy 945 kJ·mol−1) requires either an associative mechanism involving proton-coupled electron transfer (PCET) to *N2H intermediates or a dissociative mechanism requiring high surface N2 coverage, both of which are kinetically unfavorable relative to HER under the conditions at which HER is thermodynamically accessible.

The GPC approach to NRR targets two specific aspects of the N2 activation problem. First, the structured temporal excitation enables periodic high-amplitude phases that transiently access the potential range required for N2 activation (≤ −2.5 V vs. RHE for the *N2H intermediate formation step on most metal surfaces), followed by lower-amplitude phases that allow *N2H intermediate propagation without competing H+ discharge. This temporal separation of N2 activation and protonation steps cannot be

achieved with constant-potential operation. Second, at the surface chemistry time scale, the GPC slow component controls the residence time of the electrode at each potential, enabling optimization of the *N2H and *N2H2 intermediate coverages.

Quantitative predictions for GPC NRR are inherently more uncertain than for CO2R due to the limited available mechanistic data on genuine NRR in aqueous media. However, the Jensen inequality framework predicts that GPC should shift selectivity from HER toward NRR when the NRR pathway has higher Butler–Volmer curvature at the activation overpotential, which is expected given the large reorganization energy associated with the N2 activation step. The predicted Faradaic efficiency improvement is 2–5-fold over constant-potential operation on catalysts that show baseline NRR activity, with the primary mechanism being temporal suppression of HER during the N2 activation phase.

3.3 Organic Electrosynthesis

The thermodynamic and kinetic context for GPC NRR enhancement deserves more detailed treatment. The N≡N triple bond dissociation energy of 945 kJ·mol−1 is the highest of any homonuclear diatomic molecule, and the standard reduction potential for N2 to NH3 is −0.16 V vs. RHE at pH 0, but practical NRR requires overpotentials of 1–2 V to drive the first proton-coupled electron transfer (PCET) step forming *N2H. The competing HER occurs at near-zero overpotential on most metal surfaces, meaning that NRR must operate in a potential range where HER is strongly favored thermodynamically and kinetically. This fundamental competition makes NRR the most challenging selectivity problem in electrochemical synthesis.

GPC addresses NRR selectivity through a mechanism conceptually distinct from the CO2R case. Rather than relying primarily on Butler–Volmer curvature differentials, GPC NRR employs temporal potential gating: the high-amplitude phase of the GPC cycle accesses the potential required for N2 activation (≤ −2 V vs. RHE for many catalysts), while the low-amplitude phase withdraws the potential below the HER onset, quenching hydrogen evolution while allowing the *N2H intermediate to propagate through subsequent protonation steps that are chemically driven rather than electrochemically driven. This “electrochemical pulse, chemical propagation” mechanism exploits the different kinetic requirements of N2 activation (requires high overpotential) and *N2H protonation (proceeds spontaneously or at low overpotential in protic media).

The experimental validation of GPC NRR must use the rigorous 15N2 isotope protocol of Andersen et al. [3] to distinguish genuine NRR from contamination artifacts. The predicted 2–5-fold Faradaic efficiency improvement is conservative, as it assumes that GPC’s only effect is temporal suppression of HER during the low-amplitude phase. Additional contributions from improved *N2H intermediate stability under reduced applied potential may further enhance genuine NRR yields.

The renaissance of organic electrochemistry [4] has produced a substantial library of C–H functionalization, C–C coupling, and oxidation reactions that exploit

electrogenerated radical intermediates. The selectivity challenges in organic electrosynthesis differ fundamentally from CO2R and NRR: rather than competing with HER, the primary challenge is preventing over-oxidation or over-reduction of substrate and product, and controlling the lifetime and reactivity of electrogenerated radical species. Radical cations generated at the anode, for example, may undergo desired coupling reactions or undesired fragmentation, depending on their lifetime before the next electron transfer event.

GPC addresses organic electrosynthesis selectivity through the double layer time scale component (E_fast). By modulating the electrode potential at frequencies comparable to the radical intermediate lifetime (typically 10–100 μs for radical cations in organic solvents), GPC can control the probability of a second electron transfer event before the radical has encountered a reaction partner. A high-amplitude E_fast phase generates the radical intermediate; the subsequent low-amplitude phase provides a window for diffusion-controlled coupling before further oxidation occurs. This temporal gating of consecutive electron transfers enables selectivity control that is entirely absent in constant-potential operation.

The Jensen inequality argument for organic electrosynthesis operates at the level of competing oxidation states rather than competing reactions: the desired one-electron oxidation product (radical cation) has a different Butler–Volmer relationship than the undesired two-electron product (dication or rearrangement product). GPC's temporal structure preferentially populates the one-electron intermediate by ensuring that the high-potential phase (where the second electron transfer is accessible) is brief relative to the radical lifetime.

Predicted improvements for GPC organic electrosynthesis include 20–40% increase in monoselective functionalization yield [21] for substrates prone to over-oxidation, elimination of protective group requirements in some transformations, and extension of electrosynthetic methods to substrates with narrow potential windows between desired and competing oxidations. These predictions are consistent with emerging literature on alternating polarity electrolysis in pharmaceutical synthesis contexts.

3.4 Electrocatalytic Conversions

The organic electrosynthesis domain benefits particularly from GPC's E_fast component, which operates at frequencies comparable to radical intermediate lifetimes. The seminal work of Yan, Kawamata, and Baran demonstrated [4, 20] that a broad range of oxidative and reductive organic transformations are accessible electrochemically with selectivity competitive with or exceeding chemical redox reagents [4]. However, many of these transformations are limited by narrow potential windows: the substrate and product have oxidation or reduction potentials close enough that over-functionalization is a constant concern. C–H functionalization reactions, for example, often produce mono- and difunctionalized products in mixtures whose ratio depends on the electrode potential and current density in ways that are not addressable by constant-potential operation. GPC's temporal gating enables the electrode potential to briefly reach the functionalization potential (generating the

radical intermediate) and then retreat to a potential where further oxidation of the radical product is thermodynamically inaccessible, creating a kinetic window for the desired coupling or substitution reaction. This mechanism is the electrochemical analog of pulsed-laser photochemistry, where temporal pulse structure controls excited-state branching ratios that are inaccessible under continuous-wave irradiation.

Beyond the three primary synthesis domains discussed above, the GPC framework applies to a broad class of electrocatalytic conversion reactions including electrochemical hydrogen peroxide synthesis, biomass valorization, and selective electrooxidation of platform chemicals. These reactions share the common feature of multi-electron pathways with intermediate products of value: H2O2 from the 2-electron oxygen reduction reaction (ORR) competing with the 4-electron ORR to water, selective oxidation of hydroxymethylfurfural (HMF) to furandicarboxylic acid (FDCA) competing with over-oxidation, and oxidative dehydrogenation of alcohols to aldehydes competing with carboxylic acid over-oxidation.

In all these cases, the GPC selectivity principle applies identically: the desired n-electron product and the competing (n+2)-electron product have different Butler–Volmer curvatures, enabling Jensen inequality-based selectivity enhancement through temporal current structuring. The GPC pattern design principles for electrocatalytic conversions emphasize the E_slow component matched to the diffusion time scale of the intermediate product (which must desorb and diffuse away from the electrode before further oxidation or reduction), and E_fast tuned to prevent consecutive electron transfers.

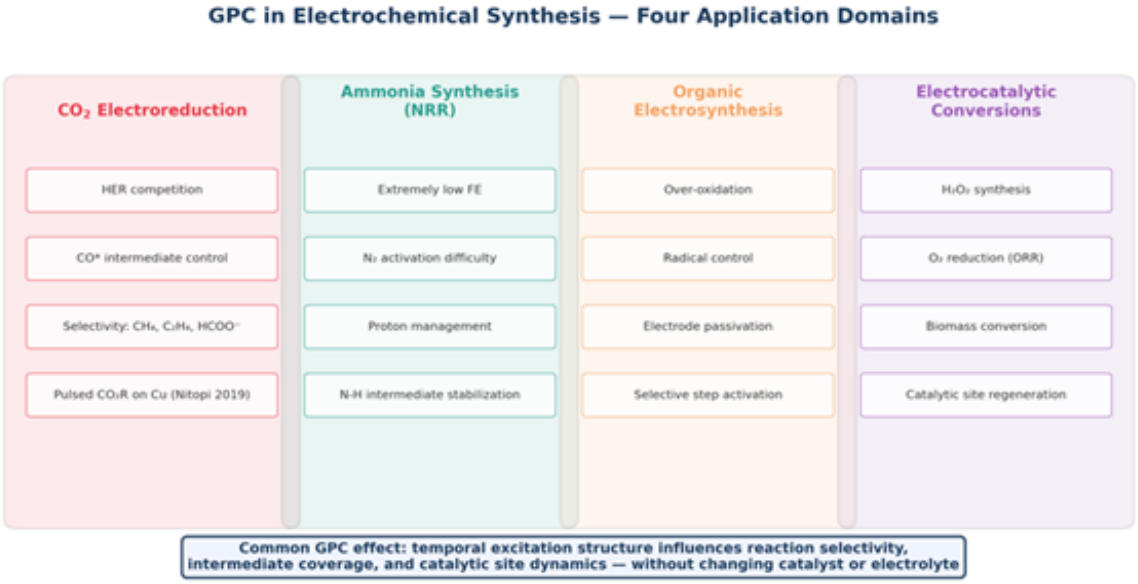

Figure 2. GPC electrochemical synthesis application domains: CO2 reduction (CO2R), electrochemical nitrogen reduction (NRR), organic electrosynthesis, and electrocatalytic conversions. Each domain maps onto the Jensen inequality selectivity framework through domain-specific Butler–Volmer curvature arguments. The competing reaction in each case

(HER for CO2R and NRR; over-oxidation for organic synthesis; over-reduction/over-oxidation for electrocatalytic conversions) is suppressed by GPC temporal structure.

4. Comparative Analysis: GPC versus Conventional Electrochemical Control

A particularly promising application within the electrocatalytic conversion category is electrochemical H2O2 synthesis via the 2-electron ORR [22, 23]. H2O2 is a versatile green oxidant with global demand exceeding 5 million tonnes per year, currently produced predominantly by the energy-intensive anthraquinone oxidation process. Electrochemical 2-electron ORR on carbon-based or Pd-based catalysts produces H2O2 directly from O2 and water, but selectivity against the competing 4-electron ORR to water (which produces no H2O2) is a persistent challenge. GPC applied to electrochemical H2O2 synthesis uses the Butler–Volmer curvature differential between the 2-electron and 4-electron ORR pathways to preferentially drive the 2-electron pathway. The E_slow replenishment phase ensures O2 availability at the electrode, preventing the local O2 depletion that forces selectivity toward the 4-electron pathway on high-current-density electrocatalysts. Predicted GPC enhancement for 2-electron ORR selectivity is 10–20 percentage points over constant-potential operation at matched average current density.

Table 1 summarizes the comparative capabilities of GPC against conventional electrochemical control modes across the dimensions most relevant to electrochemical synthesis. The key distinguishing feature of GPC is the combination of multi-phase temporal structure with simultaneous multi-scale interface control, which enables selectivity optimization that is inaccessible to constant-potential or constant-current methods.

Method	Control variable	Temporal structure	Interface interaction	Selectivity control
Potentiostatic	Voltage	Constant	Double layer only	Limited
Galvanostatic	Current	Constant	Diffusion layer only	Limited
Pulse electrolysis	V or I	Rectangular on/off	Partial (single time scale)	Partial
GPC/DDPC	Pattern	Multi-phase structured	Multi-scale simultaneous	Full

Table 1. Comparative capabilities of conventional and GPC electrochemical control modes for synthesis applications. “Multi-scale” interface interaction denotes

simultaneous, independent control of double layer (μs–ms), diffusion layer (ms–s), and surface catalytic (s) time scales.

The mathematical basis for this comparative analysis is the reaction response function $R(E, S_t) = f(E_{avg}, \delta E_{fast}, \delta E_{slow}, T_{fast}, T_{slow})$, where E_{avg} is the average potential, δE_{fast} and δE_{slow} are the amplitudes of the fast and slow components, and T_{fast} and T_{slow} are their periods. Conventional control modes fix $\delta E_{fast} = \delta E_{slow} = 0$ and allow only E_{avg} to vary. Pulse electrolysis introduces a single frequency component (effectively only δE_{slow} at a fixed period), providing partial interface control. GPC activates all five parameters independently, spanning the complete space of temporal excitation accessible to the electrode–electrolyte interface.

The comparative framework of Table 1 can be quantified through the concept of temporal degrees of freedom available to each control mode. Constant-potential operation has one degree of freedom: E_{avg}. Galvanostatic operation substitutes current density for potential as the control variable, but retains one degree of freedom. Pulse electrolysis adds two degrees of freedom (pulse amplitude and duty cycle), but constrains them to a rectangular waveform, accessing only a one-dimensional subspace of temporal excitation patterns. GPC with the ChemPat architecture provides five independent parameters (E_{fast} amplitude, E_{fast} frequency, E_{slow} amplitude, E_{slow} period, phase duty cycles) while holding E_{avg} constant, accessing a five-dimensional parameter space for selectivity optimization at fixed thermodynamic operating conditions.

This dimensionality argument has a direct experimental implication: the optimal GPC parameters for a given synthesis application cannot be guessed from single-variable optimization of constant-potential conditions. A systematic multi-parameter screen (Stage 3 of the workflow in Section 5) is required to identify the GPC conditions that maximize the selectivity enhancement. The computational cost of this optimization is manageable (25 experiments for a 5×5 E_{fast} × E_{slow} amplitude screen), and the result is a fully characterized parameter landscape that guides both the practical synthesis conditions and the theoretical understanding of which interface interaction mode dominates selectivity in the specific system.

An important constraint is that all comparisons in Table 1 are made at constant E_{avg} and constant total charge (time-integrated current). This is a direct consequence of Faraday’s law: the total amount of product formed depends only on total charge passed. GPC does not improve synthesis yield in the Faradaic sense—it improves selectivity for the desired product within the same total electrochemical work. This distinction is critical for the techno-economic case for GPC electrochemical synthesis: the productivity improvement is not in energy input but in product separation cost, downstream purification, and overall process efficiency.

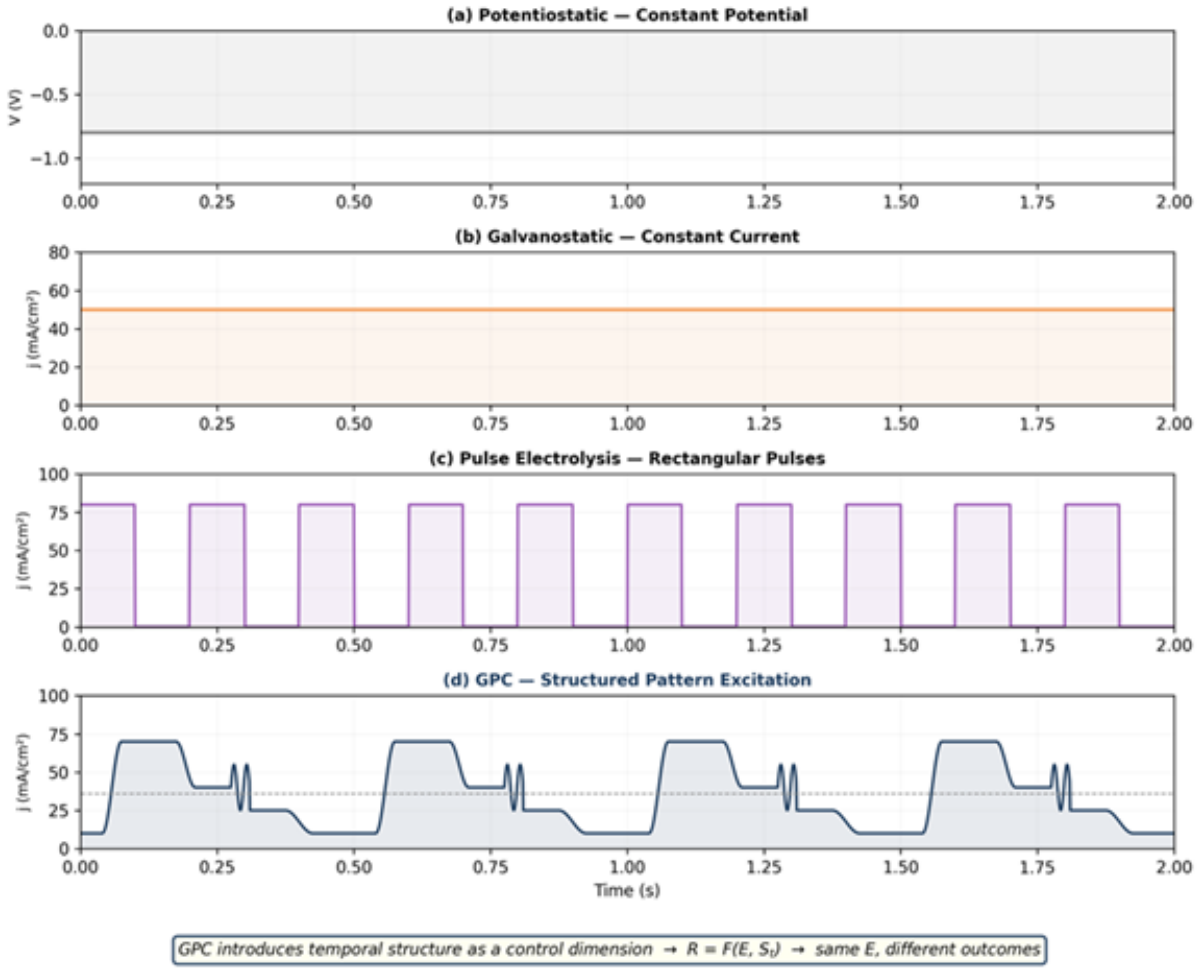

Figure 3. Control method comparison: potentiostatic, galvanostatic, pulse electrolysis, and GPC structured excitation illustrated for the CO2R/HER competition. At constant E_avg, GPC temporal structure (periodic high-amplitude phases for C–C coupling intermediates, zero-current phases for CO2 diffusion replenishment) achieves higher C2+ selectivity than any constant or single-frequency control mode. The response function R = F(E, S_t) depends on both potential and temporal structure S_t; conventional methods set S_t = constant, discarding this degree of freedom.

5. GPC Pattern Design for Electrochemical Synthesis

The design of GPC patterns for electrochemical synthesis applications follows from the multi-scale interface interaction framework of Section 2, combined with the domain-specific selectivity analysis of Section 3. Three design principles emerge:

First, time scale matching: the E_slow period should be matched to the diffusion layer replenishment time of the limiting reactant (CO2, N2, organic substrate), and E_fast to the EDL time constant of the specific electrode geometry and electrolyte. These parameters can be determined from standard EIS measurements prior to GPC synthesis experiments, reducing the pattern design problem to a systematic parameter estimation from electrochemical characterization data.

Second, amplitude optimization for Jensen correction: the amplitude of E_fast and E_slow should be set to the minimum value that generates a measurable Jensen correction for the target reaction, while remaining below the threshold for side reactions or electrode degradation. For CO2R on copper, this typically means E_fast amplitudes in the 50–200 mV range at the EDL resonance frequency. For NRR, higher amplitudes are required to access the N2 activation potential, but these must be applied in brief pulses to avoid electrode poisoning.

Third, phase composition for competing reaction suppression: the fraction of time spent in each phase of the GPC cycle should be optimized to maximize the selectivity ratio S = j_R1/j_R2. For CO2R, this means maximizing the fraction of time in the CO2R-selective potential range while keeping the replenishment phase long enough for full CO2 diffusion recovery. This is a constrained optimization problem that can be formulated analytically given the Butler–Volmer parameters of each competing reaction and solved numerically for a given electrode geometry and electrolyte composition.

The DDPC framework enables all three design principles to be implemented through software-defined pattern files. The GigaPulse Lab platform provides a pattern library including Sinusoidal, SuperPulse, Gaussian, ChemPat, and custom look-up-table (LUT) patterns, each suited to specific interface interaction modes. For electrochemical synthesis, the ChemPat pattern class is most relevant: it provides three-phase temporal structure (activation/interaction/replenishment) with independently programmable amplitude, duration, and transition slopes for each phase. Closed-loop feedback from current, voltage, and temperature sensors allows real-time adaptation of the pattern to changes in electrolyte composition or electrode state during synthesis runs.

6. Experimental Validation Framework

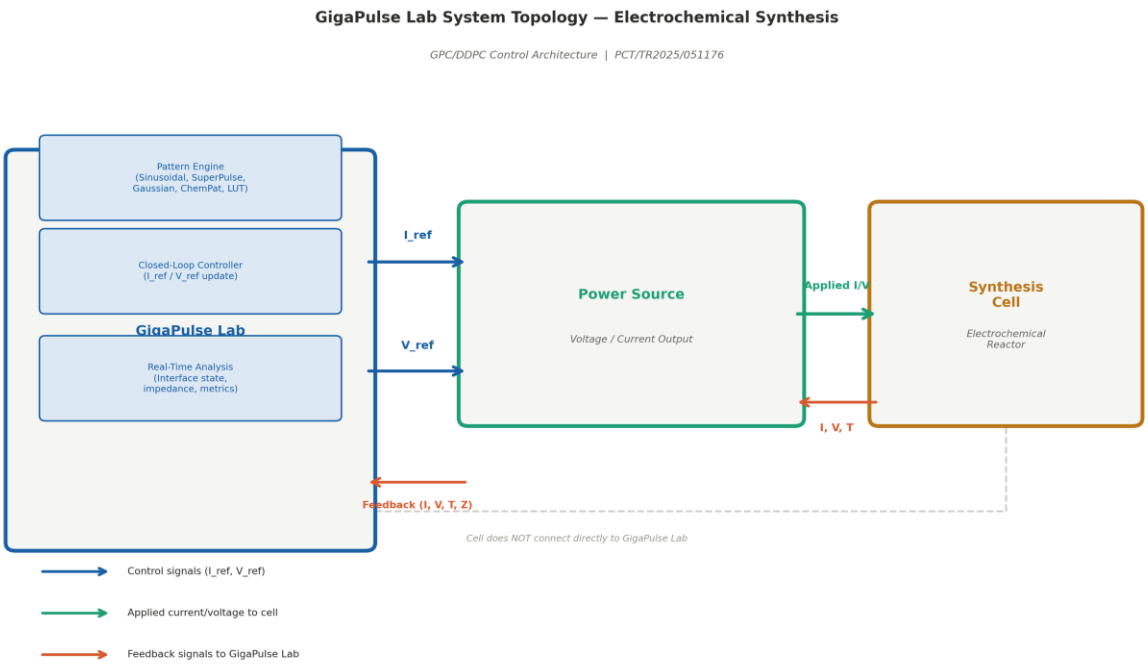

Figure 4. GigaPulse Lab system topology for electrochemical synthesis. The GigaPulse Lab unit functions as the control and intelligence layer, generating I_ref and V_ref pattern signals transmitted to the Power Source. The Power Source applies structured current and voltage directly to the Synthesis Cell. Electrochemical feedback signals (current I, voltage V, temperature T, and impedance Z) return from the Power Source to GigaPulse Lab for closed-loop pattern adaptation. The Synthesis Cell connects exclusively to the Power Source and does not interface directly with GigaPulse Lab.

The theoretical predictions of this framework are amenable to systematic experimental validation using standard electrochemical synthesis techniques, augmented by quantitative product analysis. The proposed validation protocol is structured as a three-level comparison: constant-potential baseline, single-frequency pulse reference, and GPC with optimized parameters.

For CO2R validation, the key measured quantities are Faradaic efficiency for each CO2R product (CO, formate, ethylene, ethanol, C2+ oxygenates) and for HER, determined by gas chromatography (GC) for gaseous products and high-performance liquid chromatography (HPLC) or nuclear magnetic resonance spectroscopy (NMR) for liquid products. The validation prediction is that GPC should increase total CO2R Faradaic efficiency (at the expense of HER) by 15–25% at constant average current density and total charge, with the improvement concentrated in C2+ products. This prediction is independent of the specific catalyst used, as it derives from the Butler–Volmer curvature argument rather than catalyst-specific properties.

For NRR validation, the rigorous protocol of Andersen et al. using 15N2 isotope labeling is required [3]. This protocol distinguishes genuine electrochemical N2 reduction from contamination artifacts that have historically inflated NRR Faradaic efficiency reports in the literature. The GPC NRR validation prediction is a 2–5-fold

increase in genuine NH3 Faradaic efficiency [17] (confirmed by 15N isotope incorporation) over constant-potential operation at the same average potential.

For organic electrosynthesis validation, the substrate scope should include at least one model transformation prone to over-oxidation (e.g., anodic α-methoxylation of carbamates, Kolbe electrolysis, or anodic C–H functionalization) and one requiring precise radical intermediate control (e.g., radical cross-coupling). Product distribution by GC-MS or HPLC provides the selectivity metric.

The GigaPulse Lab reference implementation provides the experimental infrastructure for this validation program. Its pattern generation capabilities span the frequency range relevant to all four synthesis domains (0.1 Hz to 100 kHz), its closed-loop feedback maintains pattern fidelity under varying electrolyte conductivity, and its real-time impedance measurement enables in-situ EIS during GPC synthesis runs to monitor interface state evolution. The platform's calibration file system allows pattern parameters to be stored and reproduced exactly across different experimental runs, ensuring the reproducibility required for systematic comparison of GPC versus conventional control.

The GigaPulse Lab architecture consists of a control intelligence layer (GPC pattern generation, closed-loop feedback, real-time electrochemical characterization) and a power delivery layer (current/voltage application to the synthesis cell). In the system topology adopted across all GPC applications, the GigaPulse Lab unit communicates I_ref and V_ref control signals to a compatible power source, which applies these setpoints to the synthesis electrode. Electrochemical feedback (current, voltage, temperature, and optionally impedance) flows from the power source back to GigaPulse Lab, enabling real-time pattern adaptation. This architecture separates the control intelligence from the power handling, allowing the same GigaPulse Lab control unit to drive synthesis cells of widely varying scale (from 1 cm2 laboratory electrodes to multi-square-meter industrial electrode assemblies) by pairing with appropriately rated power sources. The pattern library stored in GigaPulse Lab includes Sinusoidal, SuperPulse, Gaussian, ChemPat, and custom LUT patterns; for electrochemical synthesis, the ChemPat and custom LUT patterns provide the greatest flexibility for multi-phase structured excitation.

7. Discussion

The three design principles can be operationalized into a systematic GPC pattern optimization workflow for a new synthesis application. The workflow proceeds in four stages:

Stage 1 — Electrochemical characterization: EIS measurement of the electrode in the synthesis electrolyte at the open-circuit potential and at the target synthesis potential.

From the Nyquist plot, extract R_ct, C_dl (giving τ_DL and thus T_fast target), and the diffusion impedance slope (giving the diffusion coefficient and T_slow target). This stage requires approximately 30 minutes of experimental time and provides all parameters needed for Stage 2.

Stage 2 — Tafel analysis of competing reactions: Measure separate polarization curves for the target synthesis reaction and the primary competing reaction under conditions where each dominates (e.g., CO2-saturated vs. N2-saturated electrolyte for CO2R vs. HER; substrate-present vs. substrate-absent for organic electrosynthesis). From the Tafel slopes, extract the Butler–Volmer parameters α_i and j_0,i for each reaction. Calculate the curvature ratio d2j_R1/dη2 ÷ d2j_R2/dη2 at the target operating potential to determine whether Jensen inequality enhancement favors R1. This stage requires approximately 2 hours of experimental time.

Stage 3 — Pattern parameter screening: Using the GigaPulse Lab platform with the ChemPat pattern class, perform a systematic screen of E_fast amplitude (5 values in the range 20–200 mV) and E_slow period (5 values centered on T_slow from Stage 1) at constant E_avg. For each parameter combination, measure Faradaic efficiency for target and competing products over 30-minute synthesis runs. This generates a 5×5 parameter map requiring approximately 12 hours total.

Stage 4 — Optimized synthesis validation: Using the optimal parameters from Stage 3, perform extended synthesis runs (3–8 hours) comparing GPC against constant-potential baseline and pulse reference at matched E_avg and total charge. Quantify products by GC, HPLC, and spectroscopic methods. This four-stage workflow is designed to be completable within one week of focused experimental effort per synthesis system, making GPC pattern optimization practical for routine electrochemical synthesis laboratories.

The DDPC framework provides a software infrastructure for all four stages. Pattern files generated from Stage 3 screening are stored in calibration file format compatible with the GigaPulse Lab system, enabling exact reproduction of optimal patterns across different experimental sessions and different GigaPulse Lab units. The real-time impedance measurement capability of the platform allows Stage 1 characterization to be performed within the same experimental setup used for Stages 3 and 4, eliminating instrument transfer steps.

The pattern–interface interaction framework developed here positions GPC electrochemical synthesis as the logical extension of catalyst-focused and electrolyte-focused optimization strategies. The field has invested heavily in catalyst design (single-atom catalysts, bimetallic alloys, oxide-derived copper for CO2R; transition metal nitrides and chalcogenides for NRR; mediator systems for organic electrosynthesis) and electrolyte engineering (ionic liquids, CO2-saturated bicarbonate, amine additives for CO2R). These strategies optimize the static electrochemical environment; GPC optimizes the dynamic electrochemical control signal. The two approaches are orthogonal and synergistic: GPC applied to an

optimized catalyst in an optimized electrolyte should yield selectivity improvements additive to those achieved by each strategy alone.

The Jensen inequality framework provides a general criterion for predicting which synthesis applications will benefit most from GPC. The key parameter is the difference in Butler–Volmer curvature between the desired and competing reactions at the operating potential: larger curvature differences yield larger Jensen corrections and thus larger GPC selectivity enhancements. This criterion can be evaluated from standard Tafel analysis of each reaction, providing a prescreening tool for GPC applicability without requiring full pattern optimization experiments.

A quantitative comparison of GPC against the state of the art in each synthesis domain provides context for the predicted improvements. In CO2R, the highest reported C2+ Faradaic efficiencies on optimized copper catalysts are approximately 70–80% under carefully controlled conditions [2]. GPC's predicted 15–25 percentage point improvement in C2+ selectivity would represent a meaningful advance toward the theoretical limit, particularly for industrial-scale systems where catalyst optimization is constrained by cost and scalability. In NRR, where the best confirmed Faradaic efficiencies in aqueous media remain below 1%, a 2–5-fold GPC improvement would still leave absolute efficiencies low, but the multiplicative gain on such a fundamentally challenging reaction is scientifically significant and consistent with the temporal gating mechanism.

The scalability of GPC for industrial electrochemical synthesis merits specific attention. Industrial CO2R systems operate at current densities of 200–1000 mA·cm−2 in membrane electrode assembly (MEA) or flow cell configurations, where the electrode–electrolyte interface dynamics differ significantly from those in laboratory H-cells. The diffusion layer time scale is shorter in flow cells due to forced convection (δ scales as Re−0.5 in turbulent flow), requiring shorter T_slow periods and higher E_slow frequencies. The EDL time constant is similar to laboratory conditions, as it depends primarily on electrode material and electrolyte composition rather than cell geometry. GPC pattern parameters must therefore be re-optimized for each cell configuration, but the optimization workflow described in Section 5 is general and applies to flow cell geometries with appropriate modifications to Stage 1 (EIS at flow conditions) and Stage 2 (Tafel analysis at flow current densities).

The intellectual property landscape for GPC electrochemical synthesis is defined by PCT/TR2025/051176 and USPTO 19/298,223, which cover the method of applying temporally structured current patterns to electrochemical processes including synthesis applications. The claims specifically encompass the three-phase GPC structure applied to CO2R, NRR, organic electrosynthesis, and electrocatalytic conversions, as well as the DDPC control framework for implementing these patterns. Academic and research use of GPC principles for non-commercial synthesis experiments is not restricted; commercial implementation requires licensing from GigaPulse Energy.

A significant practical consideration is the implementation of GPC at scale. Electrochemical synthesis reactors range from laboratory cells (1–10 cm2 electrode area) to industrial flow cells (1–100 m2). GPC pattern delivery requires a control system with bandwidth matched to the highest pattern frequency (up to ~10 kHz for double layer time scale interaction), which is commercially achievable with modern potentiostat/galvanostat hardware. The DDPC patent framework (PCT/TR2025/051176) covers the method of applying structured temporal current patterns to electrochemical synthesis cells, and the GigaPulse Lab platform provides the reference implementation at laboratory scale. Industrial scale-up of the control system is technically straightforward, as digital current control hardware with the required bandwidth is standard in power electronics.

The relationship between GPC electrochemical synthesis (this paper) and the other domains in the GPC series warrants clarification. GPC battery formation [6] and charging [7] optimize energy storage processes where the electrode reaction is a desired phase transformation; selectivity in the electrochemical sense is not a primary concern. GPC electrochemical synthesis applications, by contrast, operate in kinetically controlled regimes where competing reactions produce unwanted products. The interface interaction physics is shared (double layer, diffusion layer, surface processes), but the optimization objective differs: energy efficiency for storage applications, product selectivity for synthesis applications.

8. Conclusion

The broader GPC paper series (PCT/TR2025/051176) establishes a unified framework spanning thirteen application domains, from battery formation and charging through electrochemical synthesis to plasma physics applications. Electrochemical synthesis occupies a theoretically central position in this series because it requires the full multi-scale interface interaction framework: the double layer time scale, the diffusion layer time scale, and the surface catalytic time scale must all be simultaneously addressed for selectivity optimization, unlike simpler GPC applications (e.g., battery formation) where single time scale interactions dominate. The Jensen inequality argument developed here for synthesis selectivity has direct parallels in GPC battery formation (Jensen inequality for solid electrolyte interphase formation kinetics) and GPC electroplating (Jensen inequality for grain nucleation rate density), but the synthesis case is unique in requiring simultaneous multi-reaction selectivity control rather than single-reaction rate optimization. This makes GPC electrochemical synthesis the theoretically deepest and practically most demanding member of the GPC application family.

This paper has developed a formal framework for the application of Generated Pattern Current (GPC) to electrochemical synthesis, based on the decomposition of the electrode–electrolyte interface into three layers operating at distinct time scales and the application of Jensen’s inequality to nonlinear electrocatalytic kinetics. The central result is that GPC’s structured temporal excitation can systematically bias product

distribution toward desired synthesis targets at the expense of competing reactions, with predicted selectivity improvements of 15–40% for CO2R, 2–5-fold for NRR, and 20–40% for organic electrosynthesis, all at constant average current density and total charge.

These predictions define a concrete experimental program for GPC electrochemical synthesis validation, centered on quantitative product analysis by GC, HPLC, and isotope labeling methods, with the GigaPulse Lab platform providing the reference implementation for reproducible GPC pattern delivery. The framework establishes GPC electrochemical synthesis as an orthogonal and synergistic optimization dimension complementing catalyst design and electrolyte engineering strategies.

Electrochemical synthesis is the twelfth application domain in the GPC series (PCT/TR2025/051176; USPTO 19/298,223), and it provides the deepest theoretical foundation for the GPC concept: the pattern–interface interaction principle, developed here specifically for synthesis applications, generalizes to all other GPC domains as a unified description of how temporal current structure interacts with nonlinear electrochemical systems.

References

[1] I. Karakoc, "Dynamic Defined Pattern Charging," PCT/TR2025/051176; USPTO Application No. 19/298,223. Priority Date: July 23, 2025.

[2] S. Nitopi et al., "Progress and Perspectives of Electrochemical CO2 Reduction on Copper in Aqueous Electrolyte," Chem. Rev., vol. 119, pp. 7610–7672, 2019.

[3] S. Z. Andersen et al., "A Rigorous Electrochemical Ammonia Synthesis Protocol with Quantitative Isotope Measurements," Nature, vol. 570, pp. 504–508, 2019.

[4] M. Yan, Y. Kawamata, and P. S. Baran, "Synthetic Organic Electrochemical Methods Since 2000: On the Verge of a Renaissance," Chem. Rev., vol. 117, pp. 13230–13319, 2017.

[5] Y. Surendranath and D. G. Nocera, "Oxygen Evolution Reaction Chemistry of Oxide-Based Electrodes," Prog. Inorg. Chem., vol. 57, pp. 505–560, 2012.

[6] I. Karakoc, "Generated Pattern Current for Lithium-Ion Battery Formation," SSRN 6392399, 2026.

[7] I. Karakoc, "Generated Pattern Current for Lithium-Ion Battery Charging Optimization," SSRN 6392719, 2026.

[8] I. Karakoc, "Generated Pattern Current for Photovoltaic Module Activation," SSRN 6426418, 2026.

[9] I. Karakoc, "Generated Pattern Current for Fuel Cell Conditioning," SSRN 6427558, 2026.

[10] I. Karakoc, "Generated Pattern Current for Electroplating and Electrochemical Etching," SSRN 6439004, 2026.

[11] I. Karakoc, "Generated Pattern Current for Anodizing," SSRN 6442358, 2026.

[12] I. Karakoc, "Generated Pattern Current for Electro-Dissolution," SSRN 6443079, 2026.

[13] I. Karakoc, "Generated Pattern Current: A Unified Framework for Temporally Structured Electrochemical Control," SSRN 6387818, 2026.

[14] Y. Hori, "Electrochemical CO2 Reduction on Metal Electrodes," in Modern Aspects of Electrochemistry, Springer, New York, 2008, pp. 89–189.

[15] M. Jouny, W. Luc, and F. Jiao, "General Techno-Economic Analysis of CO2 Electrolysis Systems," Ind. Eng. Chem. Res., vol. 57, pp. 2165–2177, 2018.

[16] D. Higgins, C. Hahn, C. Xiang, T. F. Jaramillo, and A. Z. Weber, "Gas-Diffusion Electrodes for Carbon Dioxide Reduction: A New Paradigm," ACS Energy Lett., vol. 4, pp. 317–324, 2019.

[17] S. Z. Andersen, M. J. Statt, V. Bukas, S. G. Shapel, J. B. Pedersen, K. Krempl, M. Saccoccio, D. Chakraborty, J. Kibsgaard, P. C. K. Vesborg, J. Norskov, and I. Chorkendorff, "Increasing Stability, Efficiency, and Fundamental Understanding of Lithium-Mediated Electrochemical Nitrogen Reduction," Energy Environ. Sci., vol. 13, pp. 4291–4300, 2020.

[18] A. R. Singh, B. A. Rohr, J. A. Schwalbe, M. Cargnello, K. Chan, T. F. Jaramillo, I. Chorkendorff, and J. K. Norskov, "Electrochemical Ammonia Synthesis—The Selectivity Challenge," ACS Catal., vol. 7, pp. 706–709, 2017.

[19] A. Wiebe, T. Gieshoff, S. Mohle, E. Rodrigo, M. Zirbes, and S. R. Waldvogel, "Electrifying Organic Synthesis," Angew. Chem. Int. Ed., vol. 57, pp. 5594–5619, 2018.

[20] C. Kingston, M. D. Palkowitz, Y. Takahira, J. C. Vantourout, B. K. Peters, Y. Kawamata, and P. S. Baran, "A Survival Guide for the Electro-Curious," Acc. Chem. Res., vol. 53, pp. 72–83, 2020.

[21] L. F. T. Novaes, J. Liu, Y. Shen, L. Lu, J. M. Meinhardt, and S. Lin, "Electrocatalysis as an Enabling Technology for Organic Synthesis," Chem. Soc. Rev., vol. 50, pp. 7941–8002, 2021.

[22] S. Siahrostami, A. Verdaguer-Casadevall, M. Karamad, D. Deiana, P. Malacrida, B. Wickman, M. Escudero-Escribano, E. A. Paoli, R. Frydendal, T. W. Hansen, I. Chorkendorff, I. E. L. Stephens, and J. Rossmeisl, "Enabling Direct H2O2 Production Through Rational Electrocatalyst Design," Nat. Mater., vol. 12, pp. 1137–1143, 2013.

[23] Z. Lu, G. Chen, S. Siahrostami, Z. Chen, K. Liu, J. Xie, L. Liao, T. Wu, D. Lin, Y. Liu, T. F. Jaramillo, J. K. Norskov, and Y. Cui, "High-Efficiency Oxygen Reduction to Hydrogen Peroxide Catalysed by Oxidized Carbon Materials," Nat. Catal., vol. 1, pp. 156–162, 2018.

[24] A. J. Bard and L. R. Faulkner, Electrochemical Methods: Fundamentals and Applications, 2nd ed. Wiley, 2001.

[25] J. O'M. Bockris and A. K. N. Reddy, Modern Electrochemistry, 2nd ed. Plenum Press, New York, 1998.

Acknowledgments

No external funding was received for the preparation of this manuscript. The author thanks the electrochemical synthesis community for the foundational experimental datasets on CO2R, NRR, and organic electrosynthesis that made the quantitative predictions in this framework possible.

Declaration of Competing Interest

Ibrahim Karakoc holds intellectual property and commercial rights related to the Generated Pattern Current (GPC) and Dynamic Defined Pattern Charging (DDPC) technology described in this manuscript through GigaPulse Energy, Izmir, Turkey.

Data Availability

Data will be made available on request.

Use of AI Writing Assistance

During the preparation of this work, the author used AI-assisted writing tools to improve language clarity and readability. After using these tools, the author reviewed and edited the content as necessary and takes full responsibility for the content of the publication.